

60220
U S ARMY NATICK LABORATORIES

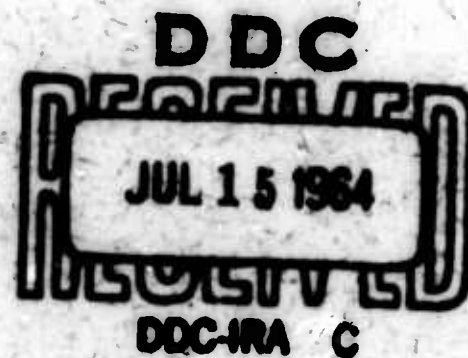
44-
TECHNICAL REPORT

PR-10

#125-

SOME EFFECTS OF JET-COMPRESSOR GEOMETRY ON EFFICIENCY
COMPRESSION-RATIO CURVES WITH TWO MAXIMA

DDC INFORMATION NOTICE
DETAILED REQUESTORS MAY OBTAIN
COPIES OF THIS REPORT FROM DDC



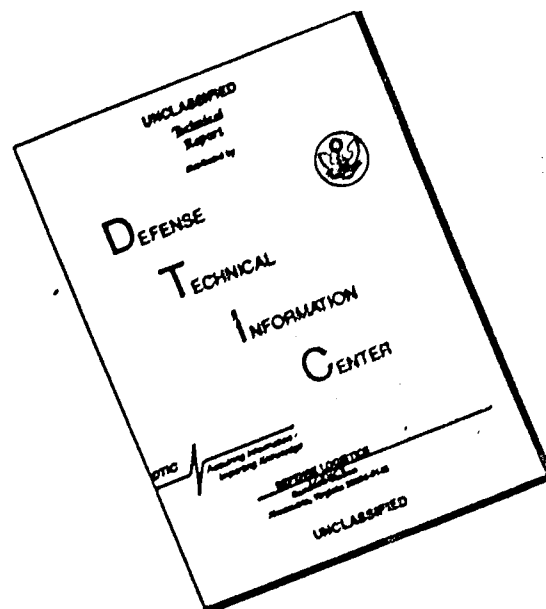
PIONEERING RESEARCH DIVISION



JUNE 1964

NATICK, MASSACHUSETTS

DISCLAIMER NOTICE



THIS DOCUMENT IS BEST QUALITY AVAILABLE. THE COPY FURNISHED TO DTIC CONTAINED A SIGNIFICANT NUMBER OF PAGES WHICH DO NOT REPRODUCE LEGIBLY.

U. S. ARMY NATICK LABORATORIES
Natick, Massachusetts

PIONEERING RESEARCH DIVISION

Technical Report
PR-10

SOME EFFECTS OF JET-COMPRESSOR GEOMETRY ON EFFICIENCY:
COMPRESSION-RATIO CURVES WITH TWO MAXIMA

Ronald A. Segars
Harold J. Hoge

Thermodynamics Laboratory

Project Reference:
1A0-10501-B010

June 1964

Foreword

The Pioneering Research Division has for several years been actively engaged in research designed to improve the efficiency of the jet compressor (ejector). Previous reports have dealt with such aspects of the problem as the effect of molecular weights of the two gas streams, and with maximization of the efficiency with respect to outlet pressure and entrainment ratio.

A considerable part of the present report is devoted to a discussion of the existence and possible causes of a second maximum in the compression-ratio curve. Such maxima are observed only under certain conditions and their causes are not well understood.

S. DAVID BAILEY
Director
Pioneering Research Division

Approved:

DALE H. SIELING, Ph. D.
Scientific Director

MERRILL L. TRIBE
Brigadier General, USA
Commanding

Contents

	Page
Abstract	iv
1. Nomenclature and Dimensions	1
2. Introduction	3
3. Experimental Measurements	4
Apparatus	4
Procedure. Effect of varying the outlet pressure	4
The various regimes of flow	6
Two maxima in the compression ratio	6
Incompleteness of the 4-regime picture	12
Effect of varying the entrainment ratio	12
Effect of using different gases	13
4. Momentum-Flux Balance for Run 91	13
One-dimensional calculations	17
Calculations with separation assumed	17
Friction in the mixing tube	19
Alternative methods of calculating friction	19
5. Momentum-Flux Balance for Run 210	20
6. Comparison of Momentum-Flux Data for All Runs Calculated	20
Momentum-flux losses in the mixing tube	22
Comparison of losses in two apparatuses	22
Comparison of losses in different systems of gases	24
Comparison of losses at different entrainment ratios	24
7. Efficiency as Influenced by Ejector Geometry	25
8. Conditions Associated with the Onset of Separation	26
Pressures at the mixing-tube entrance	26
Pressure ratio required to cause separation	27
Extent of separation	28

9. Regimes of Flow and the Second Maximum	28
The second maximum	29
Conditions under which second maxima are observed	31
Different manifestations of choking	31
A possible explanation	32
10. References	35

Abstract

Measurements have been made with a new jet compressor of different geometry, and are compared with previous results. Efficiencies, compression ratios, and other data are presented for 5 systems of gases (He:Freon-113, He:CO₂, air:Freon-12, air:air, and Freon-12:air). Calculations of momentum-flux balance within the mixing tube have been made, and various results presented in a previous report have been confirmed. Frictional losses in the mixing tube are shown for two different apparatuses, under several different operating conditions. The existence of two maxima in many of the curves of compression ratio versus outlet pressure is pointed out, and possible causes are discussed. A suggested cause of the second maximum is a rapid reduction of shock loss in the driving stream, as the acceleration of this stream to a relatively high supersonic velocity is suppressed.

EJECTOR COMPRESSION-RATIO CURVES WITH TWO MAXIMA: SOME EFFECTS OF EJECTOR GEOMETRY ON EFFICIENCY

1. Nomenclature and Dimensions

The nomenclature of the present report is the same as that of the previous report (1) and will not be repeated. The present report should be read with the previous report at hand.

Our plan was for the present apparatus to duplicate the first except that the mixing tube would be reduced to $2/3$ its former width and cross section, with other dimensions of the apparatus reduced only as necessary to match the mixing tube and preserve constant-area mixing. This plan was carried out, within ordinary machine-shop accuracy.

The length of the web separating the two flow channels is hard to control exactly. In the previous apparatus this web was 0.100 inch longer than intended; in the present apparatus the web was shorter than intended. In the previous apparatus the pressures P_3 and P_4 were measured 0.100 inch upstream from the end of the web, where the divergence of the driving-gas channel and the convergence of the driven-gas channel ended (except for the very small change due to the taper of the web).

If the two pressure taps with which P_3 and P_4 were measured had in the present apparatus been located at the plane where the divergence of the driving-gas channel and the convergence of the driven-gas channel ended, they would have been roughly 0.1 inch downstream from the end of the web. We were afraid the pressures might be influenced by interaction between the two streams at this cross section; hence the flow channels were moved with respect to the pressure taps, so that P_3 and P_4 were measured at the end of the web. At this cross section the driving-gas channel was still diverging slightly and the driven-gas channel was still converging slightly. The small unintended difference in conditions just described must be kept in mind when the results of the two investigations are compared.

The cross-section areas A_5 , A_6 and A_7 were calculated from their measured dimensions, and it was found that $A_5 + A_6$ was slightly greater than A_7 . Since constant-area mixing analysis was to be used, the measured values of A_5 and A_6 were both reduced by about 3 per mille so as to preserve the relation $A_5 + A_6 = A_7$. The values given in the tabulation below are the adjusted values.

Driving-fluid nozzle

width = 0.104 in.
length of converging part = 0.750 in.
length of diverging part = 0.450 in.
depth at entrance = 0.165 in.
depth at throat = 0.041 in.
depth at exit = 0.094 in.

Driven-fluid nozzle

angle with mixing tube axis = 5°
width = 0.103 in.
length of converging part = 1.100 in.
depth at entrance = 0.400 in.
depth at exit = 0.105 in.

Mixing tube

width = 0.206 in.
length = 2.950 in.
depth = 0.100 in.

Diffuser

width = 0.206 in.
length = 2.050 in.
depth at entrance = 0.100 in.
depth at exit = 0.402 in.

Pressure-tap locations

Same as in reference (1). This part of the apparatus was not modified between the two series of experiments.

$$\begin{array}{l}
 \text{Areas} \\
 A_1 = 0.0172 \text{ in.}^2 \\
 A^* = 0.00424 \text{ in.}^2 \\
 A_3 = 0.0412 \text{ in.}^2 \\
 A_5 = 0.0098 \text{ in.}^2 \\
 A_6 = 0.0108 \text{ in.}^2 \\
 A_7 = 0.0206 \text{ in.}^2 \\
 A_8 = 0.0828 \text{ in.}^2
 \end{array}$$

$$\begin{array}{l}
 \text{Area ratios} \\
 A_1/A^* = 4.06 \\
 A_3/A^* = 2.31 \\
 A_3/A_6 = 3.81 \\
 A_6/A_5 = 1.10 \\
 A_8/A_7 = 4.02
 \end{array}$$

2. Introduction

The jet compressor (ejector) has been under study in our laboratory for several years. Our goal is to understand the mixing process thoroughly, so that we can predict the conditions under which the highest efficiencies can be reached. Our last previous report (1) described results obtained with our second apparatus. It was a complete report in which the nature of the flow, the momentum-flux balance, the allocation of losses, and other items of interest were examined in detail.

In the present work, the same experimental attack was used with an apparatus of different geometry. Most of the phenomena previously observed were seen again in the present experiments. Some phenomena present in both investigations have been studied more carefully and are now discussed more fully than in the previous report.

Roughly the first third of the present report is devoted to an analysis of our new data along the lines of the previous investigation, to permit a comparison. This part of the report is condensed and draws heavily on the previous treatment. The remainder of the

report deals mainly with new material and is much more full and complete.

3. Experimental Measurements

The present study contains results for five systems (the driven gas is given first): He:Freon-113, He:CO₂, air:Freon-12, air:air, and Freon-12:air.

Apparatus. Most of the apparatus remained as described in reference (1). This was the case with the pressure taps, manometers, flow-controls, gas meters, and the vacuum pump used to induce the flow. The flat brass bar in which the flow channels were milled was new. Like the bar that it replaced, this bar was clamped between two brass plates, one of which carried the pressure taps.

Constant-area mixing was again used, that is, $A_5 + A_6 = A_7$. The depths and the bottom contours of all the flow channels were made the same as before. In the previous apparatus the size of the mixing tube was nominally 0.1 x 0.3 inch. In the present apparatus this was reduced to 0.1 x 0.2 inch. The width of the diffuser was reduced from 0.3 to 0.2 inch; the width of the driven-gas channel was reduced from 0.2 to 0.1 inch. No change was made in the driving-gas channel.

The flow channels were so located in the bar that all of the previously-used pressure taps communicated with it and were usable.

Procedure - Effect of varying the outlet pressure. Each run was made at a constant entrainment ratio. Each point of a run consisted of a set of pressure measurements. After each point the outlet pressure P_8 was changed. The compression ratio P_8/P_3 and the efficiency η were computed and plotted against outlet pressure P_8 . The compression-ratio and efficiency curves for a selected run (run 139, He:Freon-113, $\omega = 0.0066$) are shown in Fig. 1. The compression-ratio and the efficiency curves of the same run are always similar in shape; the chief difference is that the

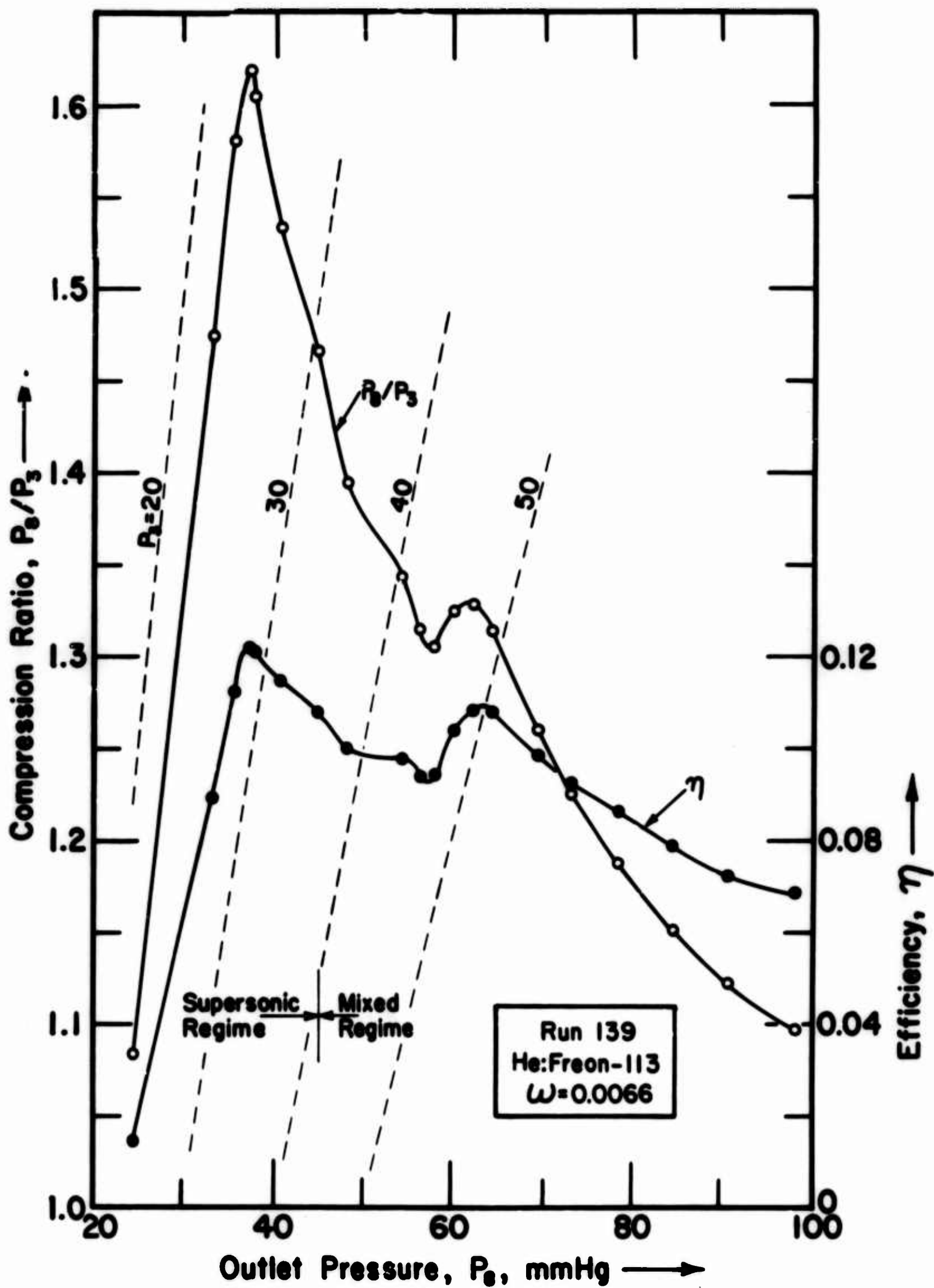


Fig. 1. Compression ratio P_0/P_3 and efficiency η as a function of outlet pressure P_0 for run 139.

ordinates of the efficiency curve experience a relative increase as P_0 increases. The curves in Fig. 1 are smooth and regular; some of the curves for other runs showed additional, sharper dips or irregularities.

The various regimes of flow. In reference (1) the four regimes of flow believed to exist in a jet compressor were described, with ideas and evidence drawn both from our own work and that of others. These regimens are (1) supersonic, (2) mixed, (3) mixed with separation, and (4) saturated supersonic. With low outlet pressure P_0 the supersonic regime is usually obtained. As P_0 is raised in a typical run, the supersonic regime is replaced by the mixed regime. As P_0 is raised further, the mixed regime yields to the mixed regime with separation. The separation here referred to takes place in the driving-gas nozzle. The saturated supersonic regime has not been realized in any of our experiments; in it the flow of driven fluid is sonic at the entrance to the mixing tube. The flow of driven fluid is therefore limited at this point and not at some cross section downstream within the mixing tube as is the case in nonsaturated supersonic flow.

In Fig. 1, the pressure at which the transition from the supersonic to the mixed regime takes place is indicated. The nearly straight rise of P_2/P_3 in the supersonic regime occurs because P_3 remains constant, isolated from P_0 by supersonic flow attached to the walls of the mixing tube. At the peak, the flow begins to detach and P_3 begins to rise, causing P_2/P_3 to fall. The transition to the mixed regime is not sharp; it occurs somewhere on the downward slope after the first maximum.

Two maxima in the compression ratio. In Fig. 1, as P_0 is raised, the compression ratio P_2/P_3 falls to a minimum after the first maximum is passed, and rises again to a second maximum. The efficiency[†] behaves in the same way. In fact, the efficiency when plotted versus the outlet pressure often showed more than two maxima. The compression ratio only occasionally showed evidence of more than two maxima. Many runs showed only a single maximum in both the compression ratio and the efficiency curves.

Since our principal interest is in efficiency, each efficiency curve was examined, and points of maximum efficiency were tabulated. The efficiencies are given in Table I, together with point numbers, compression ratios, and other relevant data for the various maxima. A few runs were made at zero entrainment; for these the efficiency is of course zero and the point of maximum P_3/P_2 has been tabulated. The arrangement is by systems (e. g. He:Freon-113), and in order of increasing entrainment ratio with each system. When there is more than one maximum at the same entrainment ratio, the arrangement is in order of increasing outlet pressure. The present experiments comprised runs 89 to 150, and 207 - 210, but runs 39, 90 and 125 are omitted from the table because of incomplete data or uncertainty in experimental conditions.

An attempt has been made to group the maxima into families. This is relatively easy in the supersonic regime; the maxima from this regime are designated by the letter S. In the mixed regime, including the mixed regime with separation, there appear to be two or perhaps three families of maxima for some systems of gases. In these cases the most important family is designated by the letter M, and the next most important by A (auxiliary system).

Auxiliary families of maxima were fairly obvious in the curves for the systems He:Freon-113 and air:Freon-12. These families are included in Table I. Some, but not all, of the additional maxima not designated S, M, or A are also included, with a question mark to indicate uncertainty as to what family they should be assigned to.

At sharp peaks, the maximum efficiency and the maximum compression ratio almost always coincide; at broad peaks the maximum compression ratio sometimes comes at one point and the maximum efficiency at the point of next higher P_3 . Except for the runs made at zero entrainment, which were mentioned earlier, all points in Table I represent peaks in the efficiency curve. Only the point or points at maxima are included, the rest of the points of

TABLE I. HIGHEST EFFICIENCIES ACHIEVED BY VARYING P_0 AT CONSTANT $\omega(\eta = \eta_{\max})$

Run & Point	\dot{m}_1 lbm hr ⁻¹	ω	η_{\max}	P_1 mm Hg	P_2 mm Hg	P_0 mm Hg	P_0/P_1	P_0/P_2	P_0/P_3	Regime
a. He:Freon-113										
141.3	2.418	0	0	152.0	14.5	34.91	.2297	2.408	.741	S
120.5	2.426	.0029	.0825	152.5	17.5	35.89	.2353	2.051	-----	S
.13	2.426	.0029	.0516	152.5	50.0	66.63	.4369	1.333	-----	M
119.4	2.426	.0049	.1112	152.5	20.0	36.08	.2366	1.804	-----	S
.14	2.426	.0049	.0822	152.5	50.0	65.82	.4316	1.316	-----	M
139.3	2.418	.0066	.1222	152.0	23.0	37.22	.2449	1.618	-----	S
.13	2.418	.0066	.1086	152.0	47.0	62.43	.4107	1.328	-----	M
122.5	2.434	.0078	.1237	153.0	25.0	37.76	.2468	1.510	-----	S
.12	2.418	.0080	.1104	152.0	39.5	52.49	.3453	1.329	-----	A
.15	2.418	.0080	.1233	152.0	47.5	62.18	.4091	1.309	-----	M
142.6	2.418	.0088	.1191	152.0	28.5	40.09	.2638	1.407	-----	S
.16	2.418	.0089	.1351	152.0	45.5	60.02	.3949	1.319	-----	M
210.5	2.405	.0090	.1173	151.2	25.7	36.54	.2417	1.422	1.159	?
.17	2.431	.0089	.1222	152.8	29.6	41.55	.2719	1.404	1.161	S
.23	2.421	.0090	.1209	152.2	40.9	53.72	.3530	1.314	1.065	A
.27	2.424	.0090	.1362	152.4	45.5	59.98	.3936	1.318	1.017	M
123.6	2.434	.0093	.1162	153.0	29.0	39.90	.2608	1.376	-----	S
.12	2.418	.0094	.1356	152.0	48.5	62.40	.4105	1.287	-----	M
140.10	2.418	.0101	.1195	152.0	40.0	51.43	.3384	1.286	-----	A
.14	2.418	.0101	.1406	152.0	48.0	61.54	.4049	1.282	-----	M
121.8	2.426	.0105	.1226	152.5	39.0	50.23	.3294	1.288	-----	A
.11	2.418	.0106	.1461	152.0	46.5	59.85	.3938	1.287	-----	M
138.6	2.434	.0122	.1268	153.0	41.0	51.25	.3350	1.250	-----	A
.10	2.410	.0123	.1592	151.5	46.5	59.10	.3901	1.271	-----	M
136.9	2.434	.0140	.1594	153.0	51.5	62.96	.4115	1.222	1.035	M
124.8	2.426	.0163	.1626	152.5	57.5	67.66	.4437	1.177	-----	M
143.9	2.418	.0185	.1684	152.0	65.5	74.68	.4913	1.140	1.023	M

TABLE I (Continued)

Run & Point	\dot{m}_1 lbm hr.	ω	η max	P_1 mm Hg	P_2 mm Hg	P_3 mmHg	P_3/P_1	P_3/P_2	P_3/P_3	Regime
a. He:Freon-113 (cont.)										
137.9	2.426	.0201	.1729	152.5	67.0	75.72	.4965	1.130	-----	M
144.9	2.418	.0215	.1655	152.0	64.0	71.94	.4733	1.124	-----	M
118.4	2.418	.0275	.1226	152.0	67.5	72.25	.4753	1.070	-----	M
b. He:CO ₂										
134.4	2.420	0	0	245.0	21.5	47.54	.1940	2.211	.931	M
131.7	2.428	.0079	.0390	250.5	38.0	61.76	.2465	1.625	1.045	M
129.10	2.428	.0151	.0610	248.0	57.5	80.74	.3256	1.404	-----	M
127.13	2.424	.0261	.0856	253.0	66.5	86.91	.3435	1.307	-----	M
128.12	2.424	.0402	.1044	245.5	90.5	107.46	.4377	1.187	-----	M
135.10	2.416	.0497	.1083	249.5	98.5	113.21	.4537	1.149	1.019	M
126.11	2.416	.0540	.1079	248.0	96.5	110.04	.4437	1.140	-----	M
130.9	2.416	.0721	.0925	252.0	108.0	117.08	.4646	1.084	-----	M
132.7	2.420	.0805	.0741	251.5	112.5	119.08	.4735	1.058	-----	M
133.6	2.416	.0873	.0563	251.0	115.5	120.15	.4787	1.040	1.030	M
c. Air:Freon-12										
207.6	2.345	0	0	176.2	13.8	39.22	.2226	2.842	.662	S
208.7	2.336	0	0	154.9	12.4	37.14	.2398	2.995	.641	S
209.3	2.334	0	0	169.7	13.6	37.88	.2232	2.786	.640	S
105.4	2.342	0	0	166.5	15.0	37.92	.2277	2.528	.738	S

TABLE I (Continued)
Run &

Point	\dot{m}_1 lbm hr ⁻¹	ω	η_{\max}	P_1 mm Hg	P_2 mm Hg	P_3 mm Hg	P_3/P_1	P_3/P_2	P_3/P_3	Regime
c. Air:Freon-12 (cont.)										
103.3	2.339	.0100	.0282	165.5	16.0	36.60	.2211	2.288	.795	S
.11	2.350	.0099	.0168	166.0	46.5	65.38	.3939	1.406	1.029	M
102.7	2.342	.0201	.0490	165.0	18.0	37.01	.2243	2.056	-----	S
91.11	2.342	.0321	.0652	166.0	22.0	39.64	.2388	1.802	1.037	S
.20	2.345	.0316	.0493	166.5	41.0	58.25	.3498	1.421	1.033	M
104.5	2.339	.0419	.0783	167.0	22.0	38.41	.2300	1.746	-----	S
.12	2.336	.0420	.0614	167.0	43.0	59.50	.3563	1.384	-----	A
.14	2.339	.0419	.0612	167.5	51.5	68.49	.4089	1.330	-----	M
106.5	2.347	.0462	.0787	165.5	23.5	38.93	.2352	1.657	1.140	S
.10	2.350	.0460	.0662	165.5	41.0	56.98	.3443	1.390	1.025	A
.13	2.347	.0459	.0666	166.0	53.0	69.80	.4205	1.317	1.036	M
93.6	2.339	.0521	.0766	162.5	25.5	39.30	.2418	1.541	1.128	S
.11	2.336	.0520	.0697	163.0	42.5	57.47	.3526	1.352	1.030	A
.13	2.339	.0519	.0704	163.0	51.5	67.06	.4114	1.302	1.031	M
92.13	2.353	.0646	.0798	164.5	40.0	53.83	.3272	1.346	-----	A
.16	2.345	.0649	.0831	165.5	55.0	70.07	.4234	1.274	-----	M
94.10	2.339	.0720	.0835	165.0	41.5	54.72	.3316	1.318	-----	A
.13	2.345	.0720	.0894	165.0	54.0	68.61	.4158	1.271	-----	M
95.5	2.336	.0799	.0820	166.0	35.5	46.86	.2823	1.320	1.070	?
.11	2.339	.0799	.0925	166.5	55.0	68.90	.4138	1.253	1.033	M
96.6	2.339	.0897	.0824	167.5	36.5	46.92	.2801	1.285	-----	?
.12	2.339	.0897	.0985	167.5	52.5	65.78	.3927	1.253	-----	M
97.12	2.339	.1052	.1030	167.5	60.5	72.58	.4333	1.200	-----	M
98.10	2.345	.1193	.1068	168.5	57.5	68.70	.4077	1.195	1.041	M
99.10	2.342	.1349	.1069	168.0	61.0	71.03	.4228	1.164	-----	M
100.7	2.339	.1494	.1055	166.5	56.0	64.92	.3899	1.159	-----	M
101.7	2.347	.1697	.0966	167.0	62.0	69.36	.4153	1.119	1.055	M

TABLE I (Continued)

Run & Point	\dot{m}_1 lbm hr ⁻¹	ω	η_{\max}	P_1 mm Hg	P_2 mm Hg	P_3 mm Hg	P_3/P_1	P_3/P_2	P_3/P_3	Regime
d. Air:Air										
117.9	2.421	0	0	334.5	30.0	62.62	.1872	2.087	.967	M
116.8	2.421	.0246	.0123	339.0	50.0	84.83	.2502	1.697	-----	M
115.9	2.425	.0501	.0222	340.5	59.0	92.66	.2721	1.570	-----	M
108.12	2.421	.0805	.0322	337.0	68.0	100.22	.2974	1.474	-----	M
107.13	2.421	.1201	.0417	339.0	80.0	110.04	.3246	1.376	1.015	M
109.14	2.413	.1600	.0490	333.5	87.5	114.74	.3440	1.311	-----	M
110.13	2.417	.1998	.0551	334.5	92.0	117.13	.3502	1.273	1.018	M
111.11	2.425	.2406	.0580	334.5	97.5	119.99	.3587	1.231	-----	M
.14	2.421	.2404	.0552	335.0	114.0	136.17	.4065	1.194	-----	A
112.9	2.421	.2798	.0582	334.5	98.5	118.19	.3533	1.200	-----	M
.12	2.421	.2798	.0563	335.5	117.0	136.73	.4075	1.169	-----	A
113.6	2.425	.3294	.0538	339.0	99.0	114.88	.3389	1.160	-----	M
.10	2.429	.3289	.0556	340.0	119.0	135.99	.4000	1.143	-----	A
114.6	2.421	.3711	.0481	342.0	105.5	118.52	.3466	1.123	-----	M
.10	2.429	.3684	.0525	342.5	119.0	133.61	.3901	1.123	-----	A
e. Freon-12:Air										
150.8	2.421	.2322	.0176	339.5	85.0	113.81	.3352	1.339	-----	M
148.6	2.421	.3476	.0215	337.0	89.0	112.92	.3351	1.269	-----	M
147.11	2.429	.4478	.0226	343.5	119.0	140.32	.4085	1.179	-----	M
149.15	2.421	.5238	.0230	340.5	113.5	132.02	.3877	1.163	1.050	M
.13	2.421	.5238	.0200	345.0	197.0	211.84	.6140	1.075	1.059	?
145.14	2.417	.5923	.0229	338.0	137.5	153.97	.4555	1.120	-----	M
146.10	2.413	.6981	.0216	338.0	141.5	154.78	.4579	1.094	-----	M

each run have been omitted to save space. Points were taken close together near maxima, so that one of the observed points would be a good approximation to the true maximum. The table contains the results of 63 runs.

Incompleteness of the four-regime picture. The general description of flow in a jet compressor given in our previous report (1), and briefly summarized above does not explain all the details of our observations. The rise of P_0/P_3 to its first maximum and its subsequent fall is explained by the transition from the supersonic regime to the mixed regime. But the existence of a second maximum, and the cause of the rise to this maximum are not obviously predicted by the 4-regime picture.

Lines of constant P_3 have been drawn in Fig. 1. When the flow is choked, so that there is no influence of downstream conditions on upstream conditions, P_3 will remain constant as P_0 rises, and the compression ratio P_0/P_3 will rise along a line of constant P_3 . In Fig. 1, the rise to the first maximum does take place along a line of constant P_3 . The rise to the second maximum is not so steep. In this region the flow behaved as if it were nearly, but not entirely choked. In some runs exhibiting second maxima there was actually a small region of true choking, in which P_3 did not change at all.

Perhaps the first question to ask is whether the second maximum in the compression ratio is associated with choking at the mixing-tube exit. This does not appear to be the case. Regimes of flow and changes in flow patterns are discussed further in section 9 of this paper.

Effect of varying the entrainment ratio. By selecting the points given in Table I, we have maximized efficiency with respect to outlet pressure, for every system and every fixed entrainment ratio studied.

We next wish to consider the entrainment ratio ω as an independent variable, and find the maximum efficiency attainable

when both P_2 and ω are varied. To accomplish this, the efficiencies η_{\max} given in Table I, and belonging to either the supersonic (S) or the mixed (M) families, have been plotted against ω in Fig. 2. This graph is similar to Fig. 5 of reference (1).

The points marked S in Table I will be found in the curves labeled S in Fig. 2, and similarly the points marked M will be found in the curves labeled M. To avoid crowding the graph, the points marked A and the points marked "?" in Table I have not been plotted in Fig. 2. However, the points of each A-family fall on a curve comparable in smoothness to the S and M curves.

Effect of using different gases. We have previously found that the molecular-weight ratio of the two gases ($W_2/W_1 = \text{driven/driving}$) has a strong influence on the efficiencies obtained. The present results fit into the same pattern. The highest efficiencies obtained for each system can be selected from those in Table I; in Fig. 2 they are of course the peaks of the various curves.

In Table II the points corresponding to these peak efficiencies are given, together with other data showing the conditions under which the maximum efficiencies were achieved. The efficiencies in this table are designated η_2 , to indicate that they are maxima found by varying two quantities independently: outlet pressure P_2 and entrainment ratio ω .

Figure 3 is a plot of some of the data given in Table II. It shows η_2 as a function of the molecular weight ratio W_2/W_1 . Appropriate data from the results of our two previous investigations have also been plotted in Fig. 3, for comparison. Comments on the effect of jet-compressor geometry on efficiency will be made later.

4. Momentum-Flux Balance for Run 91

Calculations of the equivalent momentum-flux at the entrance and exit of the mixing tube have been made for five selected runs. The equivalent momentum-flux of a stream is defined as $\dot{m}u + PA$,

Table II. Highest efficiency η_2 achieved by varying both outlet pressure P_3 and entrainment ratio ω , for each system studied.

<u>System</u>		<u>Supersonic Regime</u>				<u>Mixed Regime</u>		
(Driven:Driving)	W_3/W_1	Run & Point	ω	P_3/P_1	η_2	Run & Point	ω	P_3/P_1
a. He:Freon-113	0.02137	122.5	.0078	1.510	.1237	137.9	.0201	1.130
b. He:CO ₂	.09098	--	--	--	--	135.10	.0497	1.149
c. Air:Freon-12	.2396	106.5	.0462	1.657	.0787	99.10	.1349	1.164
d. Air:Air	1	--	--	--	--	112.9	.2798	1.200
e. Freon-12:Air	4.174	--	--	--	--	149.15	.5238	1.163
								.0230

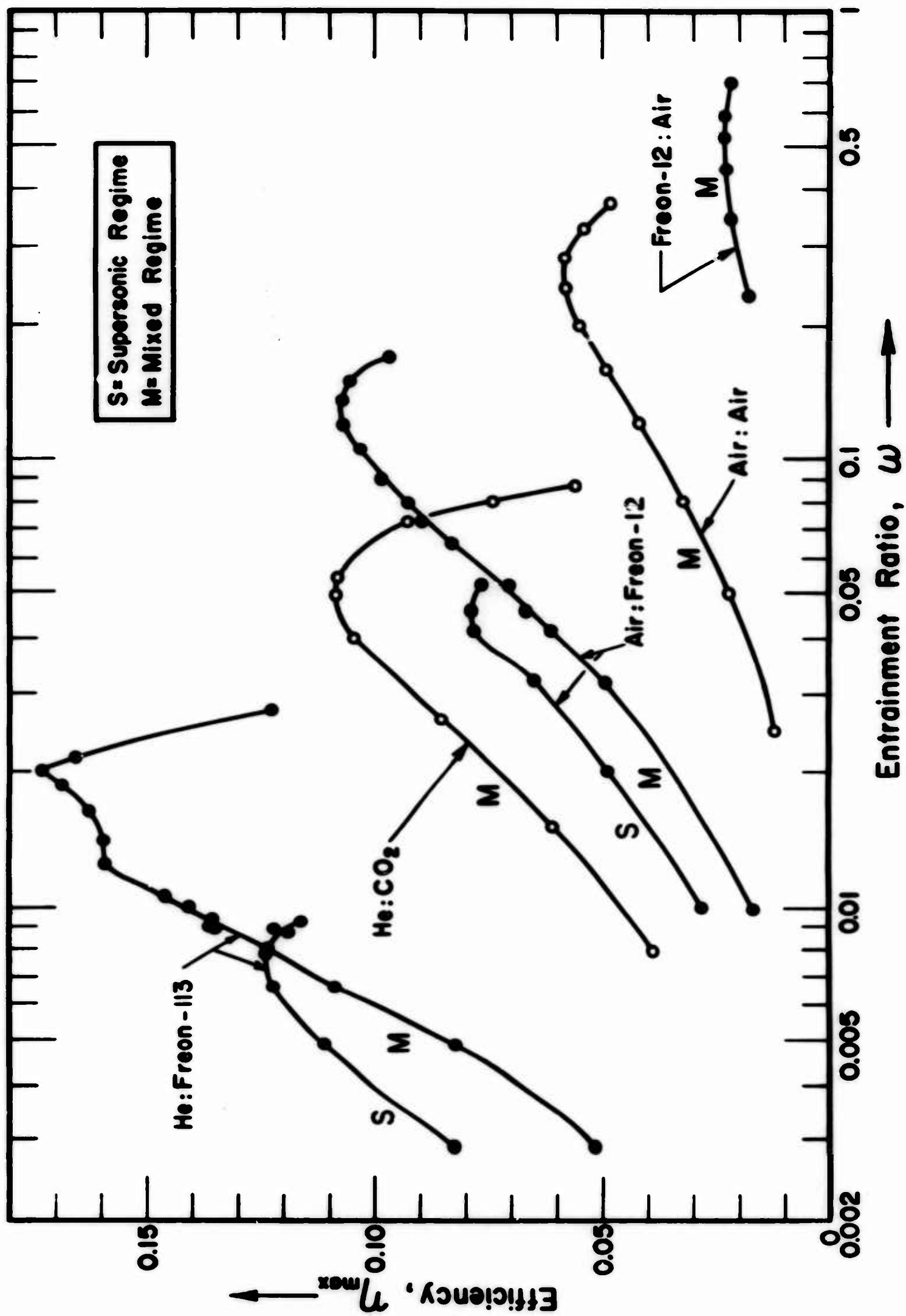


Fig. 2. Maximum efficiency (η_{\max}) versus entrainment ratio. Each plotted point is the maximum value from an efficiency curve such as the one plotted in Fig. 1.

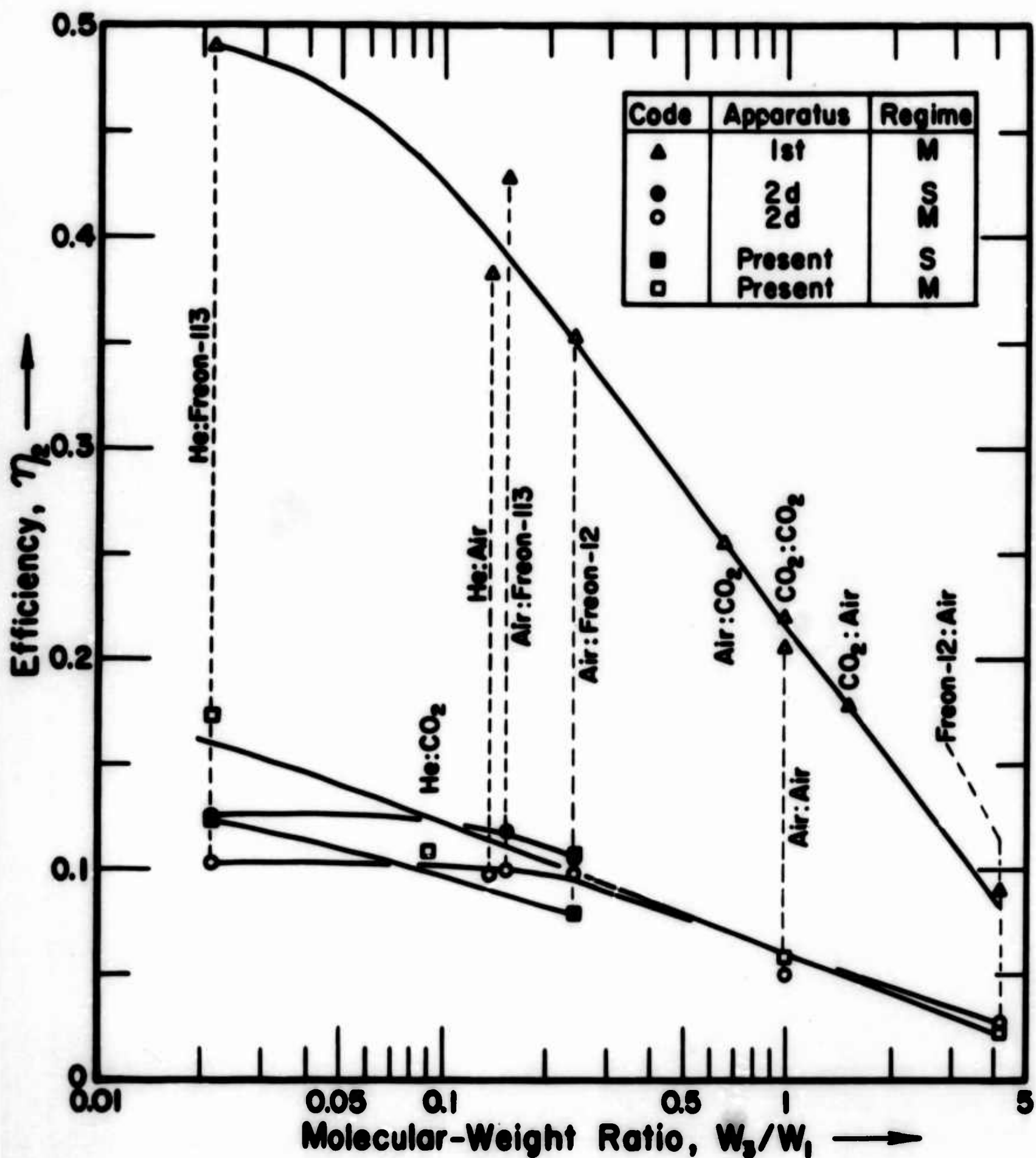


Fig. 3. Maximum efficiency versus molecular-weight ratio (driven/driving) of the gases used, for three apparatuses. Each plotted point represents the maximum efficiency found by varying both P_0 and ω .

as, in the previous report. Since the control volume is a channel of constant cross-section area, the equivalent momentum-flux at the exit should equal that at the entrance, except for friction loss. A lack of equality between input and output after friction is taken into account indicates that our model of the flow is inaccurate or insufficiently refined.

The results of calculations for run 91, a typical run on the system air:Freon-12, will now be presented, using the same methods used in reference (1). The control volume was the mixing tube; the entrance plane was that at which the two streams first made contact; the exit plane was just before the beginning of the diffuser. The velocities were calculated from the pressures observed at the channel walls, using the known stream constants.

One-dimensional calculations. The results obtained when one-dimensional theory was used are shown in Fig. 4 by the curves labeled "Uncorrected", and "Output". For low values of P_0 , the input (uncorrected) lies above the calculated output, as we know it should. But near $P_0 = 62$ mm Hg the input curve drops below the output curve. The same behavior was observed in the previous investigation.

Calculations with separation assumed. In the previous investigation, it was assumed that separation existed in the driving-gas nozzle, and a method was developed for calculating the fraction x of the nozzle outlet to which the net flow was confined. The assumption of separation increased the calculated input so that the impossible situation of output exceeding input was avoided.

The same procedure was tried for run 91, using the method of determining x that had previously been employed. Again the result was quite gratifying, as shown by the input curve in Fig. 4 labeled "With Separation". This curve forms a smooth continuation of the one-dimensional input curve from $P_0 = 42$ mm Hg upward, and parallels the output curve quite nicely.

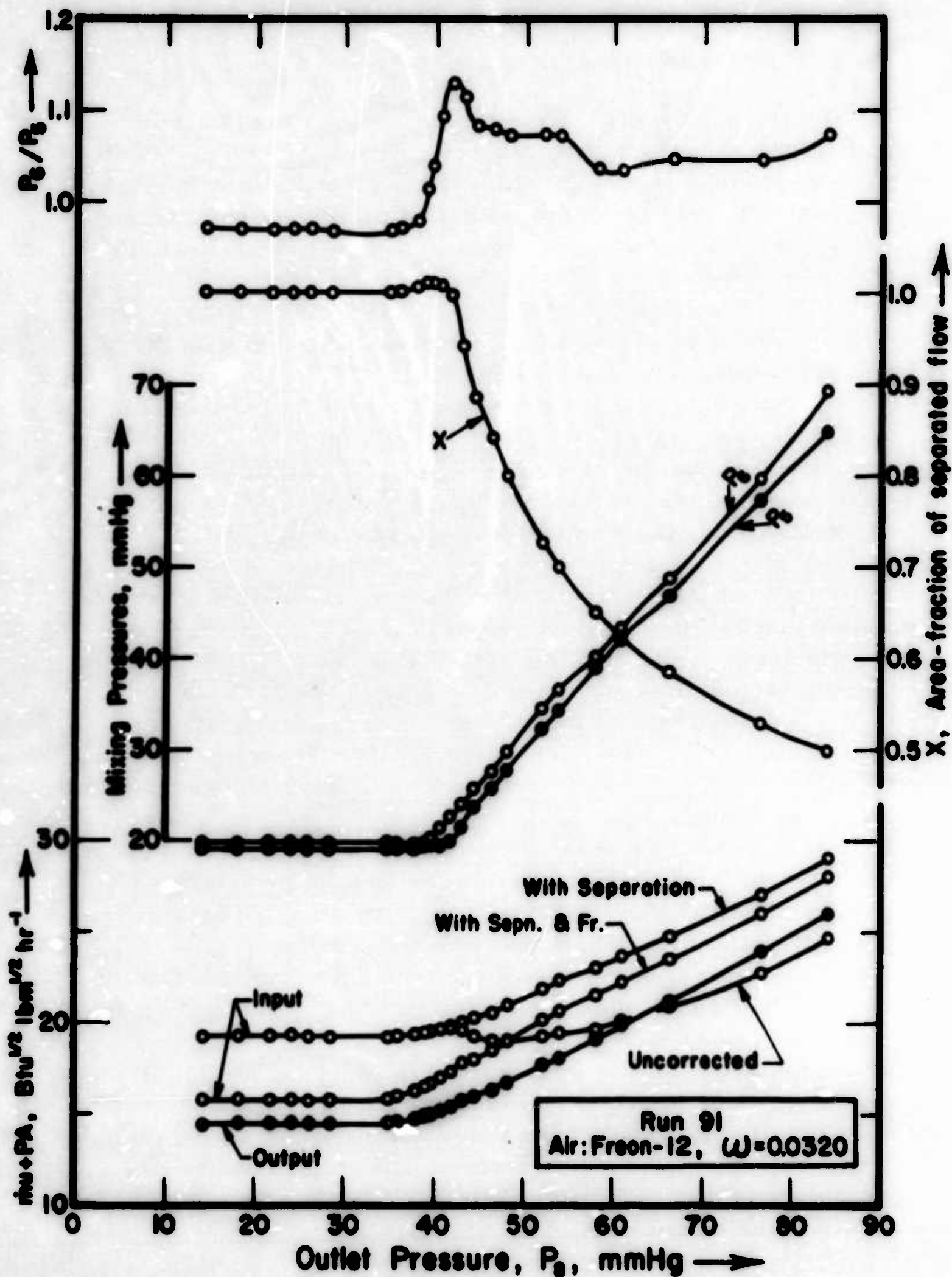


Fig. 4. Various observed or calculated quantities for run 91 as functions of outlet pressure. From bottom to top: output and input equivalent momentum flux, the latter according to various methods of calculation; pressures at the beginning of mixing, P_5 and P_6 ; fraction x of A_5 carrying the separated flow; and P_6/P_5 , the mixing-pressure ratio.

Friction in the mixing tube. It is of interest to see if the remaining difference between output and input, after separation is taken into account, can reasonably be accounted for by friction. As pointed out in the previous report (1), conditions for the calculation of friction are very poor in the mixing tube of a jet compressor. We have, nonetheless, made calculations by the methods previously described. The calculated friction loss in equivalent momentum flux has been subtracted from the calculated input; the result is plotted in Fig. 4 as the curve labeled "With Sepn. & Fr". As in reference (1) the calculated friction loss is too small to give good agreement between calculated input and output.

Alternative methods of calculating friction. Using the data of run 91, we experimented with two modified methods of calculating friction loss. One of these was a method proposed by Peters and Wehofer (2) in which the input conditions are assumed to exist throughout the first half of the mixing tube. At the middle of the tube the velocities are assumed to drop to a level where friction is negligible. This should overestimate the friction in the first half of the tube and underestimate it in the last half, and could conceivably give a correct answer for the total. Friction loss calculated in this way was on the average about equal to that shown in Fig. 4. However, the Peters and Wehofer method gave lower values of friction at low P_3 's and higher values of friction at high P_3 's than our usual method of calculation.

In the second of the modified methods of attack on the friction problem, the mixing tube, instead of being treated as a single region, was considered as made up of sections, each associated with one of the pressure taps. The velocity, Reynolds number, friction coefficient, and friction loss were computed separately for each section of the tube, and the losses were finally summed to get the total friction loss. Three points were calculated by this method: one at low P_3 , one near the onset of separation, and one at high P_3 . At the low pressure, agreement between input and output was substantially better than that given by either of the previously described methods of computing friction. At the intermediate pressure, the advantage of the method was less pronounced, and at

the high pressure there was no improvement. Since the computations are very laborious, only these three points were calculated.

5. Momentum-Flux Balance for Run 210

As a second example of the calculation of equivalent momentum-flux, run 210 will be discussed. This run is on the system He:Freon-113. All the other runs of the present investigation for which momentum-flux calculations were made were on the system air: Freon-12. Run 210 was made much later than the rest; in it 38 points (an unusually large number) were observed. For this run a cathetometer was used to measure the mercury column heights; this reduced the scattering in the observed pressures, which was ± 0.5 mm Hg when the cathetometer was not used.

The calculations for run 210 were performed in the same way as those of the preceding section. The results are shown in Fig. 5. There were so many plotted points, lying so close together, that only the smooth curves drawn through them are shown. The output and input calculated one-dimensionally cross at $P_g = 53$ mm Hg. Separation was assumed to be the cause, and a calculation involving separation was made. The four points of lowest P_g were assumed to be unaffected by separation; basing the separation correction on them the curve marked "with separation" shown in Fig. 5 was obtained. As usual, the input calculated on the basis of separation parallels the output curve satisfactorily.

The usual calculation of loss of equivalent momentum-flux within the control volume by friction was made; the result of subtracting friction from the input (corrected for separation) is shown in Fig. 5. The subtraction of friction, as usual, lowers the input curve part way to the output curve, but not far enough to give good agreement.

6. Comparison of Momentum-Flux Data for All Runs Calculated

So far, calculations of equivalent momentum-flux balance have been made for 10 selected runs. Five of these runs were made with the present apparatus: the two described above (runs 91 and 210),

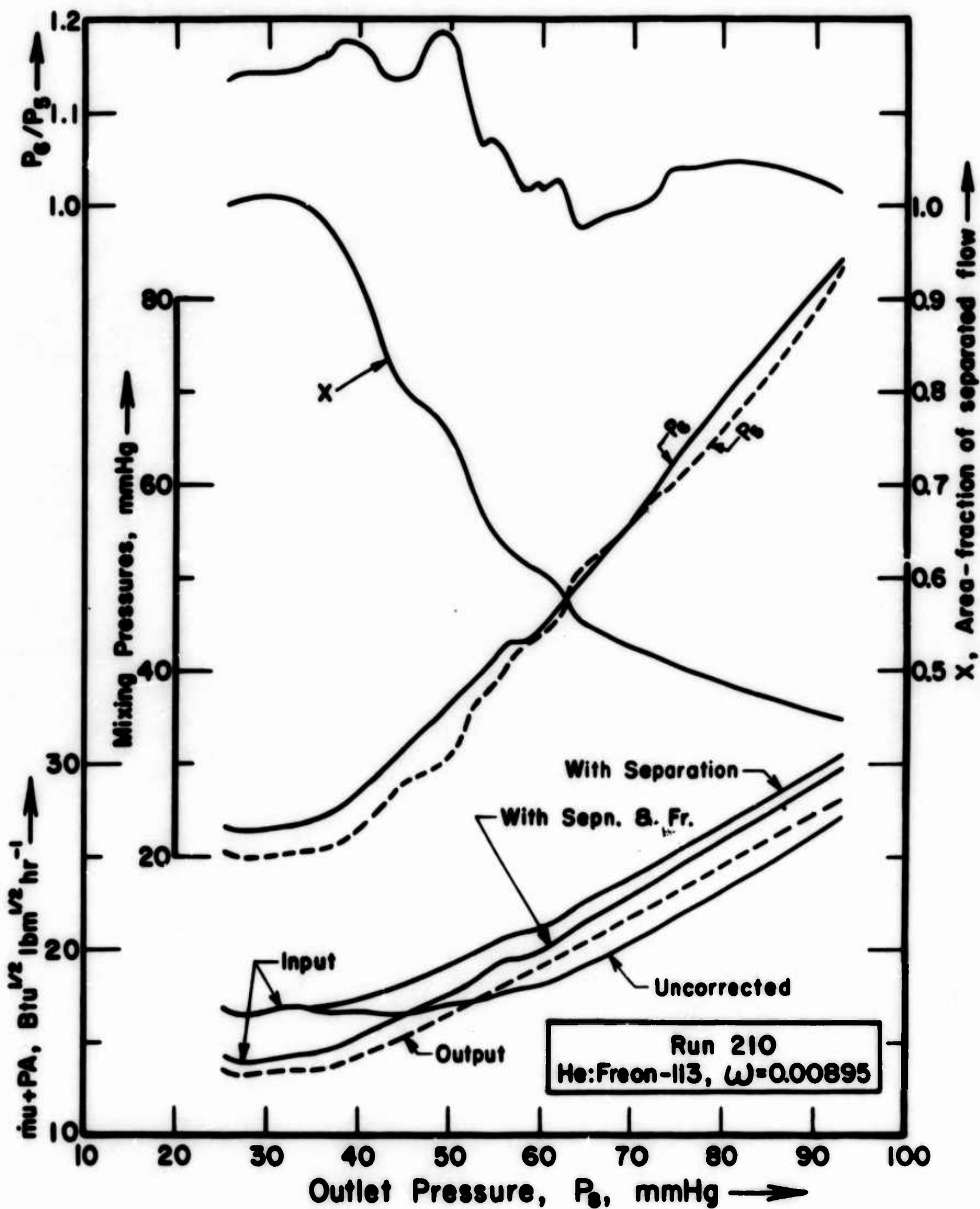


Fig. 5. This figure shows the same items as Fig. 4, but is for a different run.

plus runs 93, 98, and 105. The other five runs: 16, 19, 23, 45, and 49, were made during the previous investigation (1). In all 10 of these runs a discrepancy between calculated input and output has remained, after taking separation and friction into account. Most of this discrepancy could be removed by making a larger allowance for friction, but there is no obvious reason for increasing this allowance.

An alternative way to remove the discrepancy is to assume non-uniform flow at the exit plane of the control volume. Nonuniform velocity increases the output of equivalent momentum-flux above that of the assumed one-dimensional flow. Some studies were made to determine how much nonuniformity would be required to bring output plus friction loss up to the level of input. The nonuniformity required seems large, but we incline to the belief that substantial nonuniformity exists. Since the extent of nonuniformity is still somewhat speculative, no quantitative estimates will be given at this time.

Momentum-flux losses in the mixing tube. The 10 runs now calculated permit some conclusions to be drawn regarding losses. The equivalent momentum-flux at the control-volume exit, calculated one-dimensionally as always, has been divided by the equivalent momentum-flux at the control-volume entrance, calculated with separation assumed. The resulting ratio of output to input flux is plotted versus P_8 in Fig. 6. Note that this ratio depends on the flow-model adopted at the entrance and exit but is independent of any assumptions about friction. A high value of the ratio is desirable; it indicates a low friction loss. The figure shows that friction destroys 25 percent or more of the equivalent momentum-flux when P_8 is small and the gas velocities in the mixing tube are high; but only about 10 percent at high values of P_8 , which correspond to low velocities in the mixing tube. Unfortunately, the compression ratio P_8/P_1 falls off at high values of P_8 , so that jet compressors operating in this region are likely not to be very useful in practical applications.

Comparison of losses in two apparatuses. The only system calculated for both apparatuses was air:Freon-12. The losses were

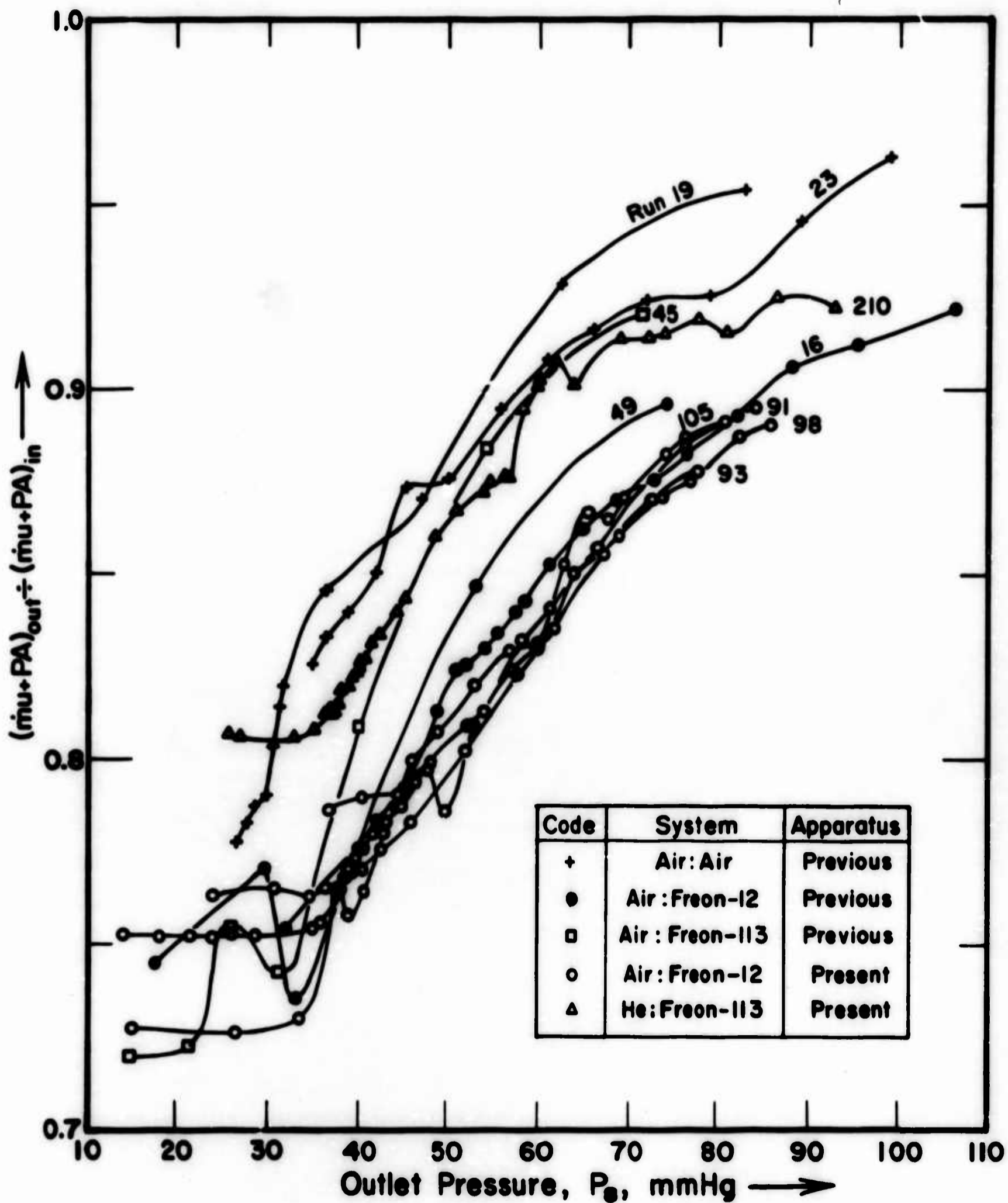


Fig. 6. Loss of equivalent momentum-flux within the mixing tube, for several systems of gases at various entrainment ratios, and for two apparatuses. The equivalent momentum-flux at the mixing-tube exit has been divided by that at the mixing-tube entrance, and the result plotted versus outlet pressure.

lower (curves are higher) for the previous apparatus than the present, though one of the two curves for the previous apparatus (run 16) crosses some of the curve for the present apparatus. ~~The basic~~ difference between the two apparatuses was that the previous had a mixing tube with dimensions nominally 0.1 x 0.3 inch, ~~whereas~~ the present was nominally 0.1 x 0.2 inch. We had expected the smaller tube to show larger friction losses; this expectation was confirmed, but not very conclusively.

Comparison of losses in different systems of gases. For the present apparatus, two systems were calculated: He:Freon-113 and air:Freon-12. The first of these systems showed the smaller losses of equivalent momentum-flux. We had expected that the heavier, and hence the slower-moving, driving gases would be found in the systems that showed the least friction loss. Such is the case for the two systems now under discussion. However, when the previous apparatus was used the situation was different. For that apparatus the systems calculated were air:Freon-113, air:Freon-12, and air:air. If the molecular weight of the driving gas is the controlling factor, we should expect the first of these three systems to show the least friction; the second should be next; and the third should show the most friction. Actually the system that should show the most friction shows the least; the other two are in the expected relative order. A comparison of this sort leaves several factors out of account; it could be refined by calculating Reynolds numbers and getting friction coefficients from them. However, this would require assumptions regarding flow patterns in the mixing tube and will not be undertaken at this time.

Comparison of losses at different entrainment ratios. Limiting our comparisons to runs on the same system and with the same apparatus, but at more than one entrainment ratio, there are three groups of runs to be examined. No pattern of dependence of friction on entrainment ratio emerges. In one case (runs 16 and 49) friction decreased as entrainment ratio increased. In another case (runs 19 and 23) the opposite occurred. In the third case (runs 91, 93, 98, and 105) friction decreased as entrainment increased, but the effects were small and uncertain in the case of runs 93 and 98.

7. Efficiency as Influenced by Ejector Geometry

The geometry of a jet compressor is much more difficult to vary than most of the other parameters that we have investigated. To vary the geometry significantly one usually has to build a new apparatus, or at least substitute some new parts in his apparatus. Three geometries have now been investigated in this laboratory, employing: (a) the present apparatus, (b) the apparatus described in reference (1), and (c) the apparatus described in reference (3). Data obtained with the last-mentioned of these are given in reference (4).

The highest efficiency attained with the present apparatus is 0.173, at a compression ratio P_3/P_2 of 1.130, using the system He:Freon-113 at an entrainment ratio of 0.0201 and operating in the mixed regime. The highest efficiency reached in the supersonic regime was $\eta = 0.124$ at a compression ratio of 1.510, using the same system at an entrainment ratio of 0.0078.

The highest efficiency reached with each system of gases, using 3 different apparatuses, is shown in Fig. 3. In the first investigation (3,4) we obtained our highest efficiencies and lowest compression ratios. In the second we got lower efficiencies and higher compression ratios. The present investigation we expected to be an additional step in the same direction; instead the present apparatus has given compression ratios and efficiencies roughly equal to those obtained in the second one. The results obtained with it have helped us to understand ejector behavior, but have not otherwise brought us much nearer to our goal of increased efficiency.

In the three geometries, the area A_3/A_2 has been progressively decreased. In the last two apparatuses, which are easiest to compare, many dimensions were left constant, but A_3 was reduced by half. The driving-fluid channels were the same in the two apparatuses, within the accuracy of ordinary machine-shop construction. The lengths of the two mixing tubes were almost equal, but the last one had only 2/3 the cross-section area of the previous one, so it had a greater length-to-area ratio. This made it easier for us to observe certain phenomena than it had been in the previous

apparatus. It is probable that a shorter mixing tube in the present apparatus would have given somewhat higher efficiencies.

Perhaps the most promising method of increasing compression ratios, and, hopefully, avoiding any loss in efficiency, is one we have not yet tried. It is to increase the expansion ratio of the driving-fluid nozzle without changing the total cross section of the mixing tube. However, there are so many interacting processes in a jet compressor that one is never quite sure what results a new apparatus will give.

8. Conditions Associated with the Onset of Separation

The pressures of the two streams of gas as they first come in contact in a jet compressor are of considerable interest. In "constant-pressure mixing" these two pressures are equal and remain so as mixing proceeds. In "under-expansion" the driving fluid has the higher pressure, and in "over-expansion" the driven fluid has the higher pressure.

Pressures at the mixing-tube entrance. Figures 4 and 5 show, for runs 91 and 210 respectively, the pressure P_5 of the driving gas, and the pressure P_6 of the driven gas, both measured by wall taps at the cross section where the two streams first come in contact. The abscissa is the outlet pressure P_8 ; in a normal run we start at low P_8 and proceed upward. As P_8 increases, P_5 and P_6 at first remain constant. In run 91 (air: Freon-12, $\alpha = 0.0320$), P_6 begins to rise almost linearly at $P_8 = 38$ mm Hg. The break in the curve of P_6 is related to the transition from the supersonic to the mixed regime, for, as discussed in (1), the supersonic regime is characterized by an independence of upstream conditions from changes in downstream conditions.

As P_8 increases above 38 mm Hg, P_6 increases with it, and at about $P_8 = 40$ mm Hg, the pressure P_5 of the driving fluid begins to rise. There is a small drop in P_5 before the rise begins, but this may be experimental error. The beginning of the rise in P_5

signals the transition from the "mixed regime" to the "mixed regime with separation". In the present instance the mixed regime (without separation) existed only between $P_8 = 38$ and $P_8 = 40$, but under other experimental conditions the regime can persist over a longer range.

In run 210 (He:Freon-113, $\omega = 0.00895$), P_5 was greater than P_6 even at the lowest values of P_8 ; this is shown in Fig. 5. The two curves were initially horizontal and parallel as we expect them to be in the supersonic regime. Departures from strictly horizontal paths are believed to be due to unsteady conditions as the run was started; the entrainment ratio was changing in this period more than usual. Near $P_8 = 63$ mm Hg, P_5 becomes larger than P_6 and remains higher until P_8 reaches about 71 mm Hg.

In run 91 a similar phenomenon occurs near $P_8 = 60$ mm Hg, but the curves of P_5 and P_6 approach each other without crossing. This behavior was observed in several other runs, but only in run 210 did the two curves actually cross. The cause of this rise in P_5 relative to P_6 is not known.

Pressure ratio required to cause separation. Referring to Figs. 4 and 5, as long as P_5 and P_6 remain constant their ratio will remain constant. This behavior is characteristic of the supersonic regime. Eventually, the increase in P_8 causes the supersonic regime to give way to the mixed regime. At this point the pressure P_5 comes into communication with P_8 and starts to rise. A little later (usually) the mixed regime gives way to the mixed regime with separation, and P_5 starts to rise along with P_6 .

The ratio P_5/P_6 is plotted for runs 91 and 210, in Figs. 4 and 5, respectively; it is the top curve in each figure. In run 210, there is no substantial rise in P_5/P_6 just before separation begins; this can be understood if we assume that separation begins almost simultaneously with the end of the supersonic regime. For run 91, the maximum value of P_5/P_6 , reached just as separation begins, is 1.126. For runs 93 and 105, the values of P_5/P_6 at the onset of

separation. Were 1.138 and 1.132 respectively. For run 98, separation was present at all values of P_0 . For run 210 the highest value occurs well after separation has begun; the somewhat lower value at the onset of separation is 1.160.

All of the values of P_6/P_5 at separation given above are quite low; other investigators have found values as high as 2.5. In our previous work (1) we also found that separation occurred at very low values of P_6/P_5 , and suggested that this might be due to the small dimensions of our apparatus, which would increase the importance of the boundary layer. If this explanation is correct, it should apply even more to the present results, for the present apparatus is still smaller than the previous one.

Above the value of P_0 at which separation begins, the curves of P_6/P_5 show some oscillations whose cause is unknown.

Extent of separation. According to our model of separation, the separated flow occupies a fraction x of the area A_5 of the driving-nozzle exit. This fraction is calculated from the observed values of P_5 , by a method described in reference (1). This method is such that the average value of x prior to separation is made equal to 1. The values of x calculated for runs 91 and 210 are shown in Figs. 4 and 5 respectively. For run 91 the curve rises slightly above 1 just before separation begins. We do not know whether to attribute this to experimental error or to some actual change in conditions. The true value of x cannot, of course, exceed 1.

The calculated values of x depend on the assumptions made and should be considered as approximate values only. Near $x = 1$ our picture may be a fairly good approximation to actual conditions, but when x is far below 1 our assumptions may be much farther from the truth.

9. Regimes of Flow and the Second Maximum

In reference (1) we described four regimes of flow in a jet

compressor: the supersonic regime, the mixed regime, the mixed regime with separation, and the saturated supersonic regime. These regimes help us to explain the processes that occur in an ejector, but the picture that they give is not yet complete.

For example, we mentioned in section 3 of this report that two maxima often occur in the curve of compression ratio (P_0/P_3) versus outlet pressure (P_0). The first maximum is explained by our 4-regime picture, but the second one is not. Our data will now be examined with respect to the 4-regime picture and attempts will be made to supplement it where necessary.

Referring to the curve of P_0/P_3 in Fig. 1, consider what happens as P_0 is raised. First there is a steep rise in the supersonic regime, while P_3 remains constant. According to our picture, the mixing tube is at some cross section entirely filled with supersonic flow. This isolates the upstream flow from the downstream flow and P_3 remains constant. At the first maximum the isolation begins to break down, and at some more or less arbitrary point on the downward slope of the peak the mixed regime is established. The coupling between P_0 and P_3 is now close; the two pressures rise together, though not necessarily at just the same rate.

Usually (in our experiments) the mixed regime without separation exists only over a narrow range of P_0 before it gives way to the mixed regime with separation. The separation occurs of course in the diverging part of the driving-gas nozzle.

The second maximum. As the outlet pressure P_0 is raised further, the compression ratio in Fig. 1 reaches a minimum value and then rises to its second maximum. Between the minimum and the second maximum the change in P_3 is quite small, as may be seen by comparing the curve with the dashed lines representing constant values of P_3 .

Additional examples of second maxima in P_0/P_3 are shown in Fig. 7. This is a reproduction of the lower part of one of our original graphs. Although some detail is not visible, a whole

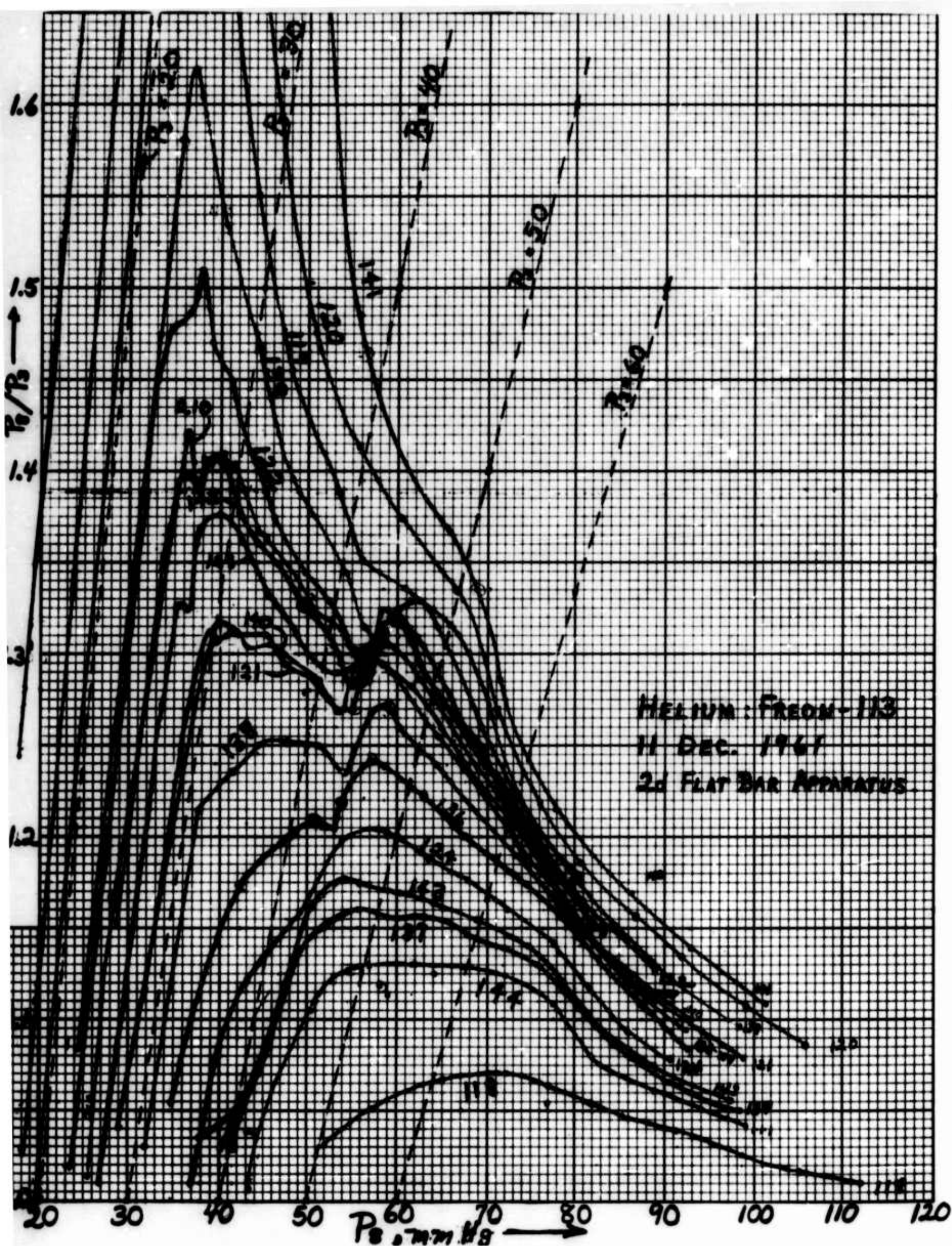


Fig. 7. Reproduction of the lower part of original graph of compression ratio versus outlet pressure, showing all runs on the system He:Freon-113. Many runs show second maxima, lying between the dashed lines $P_3 = 40$ and $P_3 = 50$.

family of second maxima may be seen near the middle of the figure. The rising portions of these lie within a narrow range of values of P_2 , ranging from 43 to 45 mm Hg. Note that the curve of P_2/P_1 shown in Fig. 1 is also included in Fig. 7.

Examples of second maxima obtained in our previous investigation may be seen in Fig. 3 of reference (1). It was, in fact, somewhat easier to obtain two maxima with the previous apparatus than with the present one. These maxima were noticed at the time of our previous work, but not much was said about their probable cause.

Conditions under which second maxima are observed. From the figure just referred to, and from Fig. 7, it may be seen that two maxima in the compression ratio are present only for an intermediate range of entrainment ratios. At very low or zero entrainment only the first maximum is present, and at high entrainment ratios only the second maximum is present.

Curves showing both maxima were most easily obtained with the systems He:Freon-113 and air:Freon-113. The system air:Freon-12 showed both maxima very plainly in the previous apparatus; in the present apparatus the runs of low entrainment showed the first maximum clearly, the runs of high entrainment showed the second maximum clearly, but only a few runs of intermediate entrainment showed both maxima. All other systems showed only faint indications, or none, of more than one maximum.

The systems showing both maxima strongly all have a small molecular-weight ratio W_2/W_1 ; these are the systems that have been found to give high ejector efficiencies. However, a favorable molecular-weight ratio does not necessarily insure that both maxima will appear. The systems He:CO₂ and He:air both have small molecular-weight ratios but do not show two maxima.

Different manifestations of choking. It was mentioned earlier that choking could be considered as a possible cause of the rise of

the compression ratio to its second maximum. Several forms of choking are already known to be present in the ejector; they will be listed so that they will not be confused with the kind of choking that may cause the second maximum. First there is choking of the flow of driving gas at the throat of the driving nozzle. Second there is, in the supersonic regime, choking of the combined flow of the two streams when the driving stream has accelerated the driven stream so that all the flow is either supersonic or sonic; we do not know at just what plane in the mixing tube this occurs. Third, there may be, in the mixed regime, choking at the exit of the mixing tube, when the outlet pressure P_8 is low enough.

The rise to the second maximum is not caused by any of the three forms of choking listed above. The second maximum occurs in the mixed regime or the mixed regime with separation, and the velocity u_7 (calculated one-dimensionally on the assumption that the two streams are fully mixed) at the mixing tube exit is typically about half of the sonic velocity c^* . Inspection of the pressures of the two streams in the region where mixing begins shows that the rise of P_6/P_3 to its second maximum is associated with a change in the pressure pattern of the driving stream. The driven stream is not much affected, at least at the points where pressure taps are located. As P_6/P_3 rises to its second maximum, the pressure P_6 at the driving-nozzle exit rises more or less steadily, but the pressure at the next station downstream (tap g) on the driving-gas side of the mixing tube, experiences an opposite change, in some cases at least.

A possible explanation. The observed behavior can be qualitatively explained if we assume that the driving stream is undergoing a shock in which its pressure rises, and that during the rise of P_6/P_3 to the second maximum the pressure ratio across this shock decreases. This weakening of the shock and reduction of shock loss will result as the plane of separation within the driving-gas nozzle is pushed upstream. We know that the loss in available energy caused by a shock decreases rapidly as the supersonic velocity approaches c^* (weak shocks are nearly isentropic). Hence if this explanation is correct the velocity u_{6x} of the separated core

flow must be supersonic, but not very much so. Our model of the separated flow permits u_{sx} to be calculated, but the model is only an approximation and the calculated values of u_{sx} may be substantially in error. However, the calculated values do not conflict with the explanation of the second maximum given above; this is considered reassuring.

Oblique shocks may be expected within the separated core of driving gas. These will originate at the plane of separation and will extend across the core. As the plane of separation is pushed upstream, an oblique shock might at first clear the web that divides the two streams and later it might be reflected by the web. While the change from one condition to the other took place, it is conceivable that P_4/P_3 could remain constant or nearly so. This picture is not plausible if the core flow has separated from the web. However, separation might occur at the bottom of the channel (which is the only diverging wall) and not at the other walls.

Effects of oblique shocks can be expected to be quite noticeable when the entire driving-nozzle outlet is supersonic, but separation is incipient, with P_4/P_3 somewhat greater than 1. This condition occurred, however, at low values of P_4 , before the second maximum was reached. Although the number of runs for which separation was actually calculated was not great, none of them showed second maxima until after separation was well established.

Since the mechanism that produces second maxima is not fully understood, we cannot assume that second maxima would be found in a jet compressor of axial symmetry; it is possible, though not probable, that the side-by-side geometry of our apparatus was important in producing the second maxima.

The nature of the mechanism that limits the flow of driven gas while the rise to the second maximum in P_4/P_3 occurs is not known. Perhaps the driven gas actually becomes sonic. Perhaps the driven fluid remains subsonic, but the combination of a subsonic and a supersonic stream side-by-side behaves like a single sonic

stream, more or less as described by Pearson, Holliday, and Smith (5).

A new bar with flow channels similar to those used in reference (1) has been built. In it the mixing tube discharges directly into a much larger channel; there is no tapered diffuser. The mixing tube can be shortened (irreversibly) by placing the bar in a milling machine and extending the large channel farther upstream. Further discussion of second maxima and flow-limiting processes will be deferred until data taken with the new apparatus are analyzed.

10. References

- 1. Harold J. Hoge and Ronald A. Segars, "Further Studies of the Jet Compressor", Tech. Rept. PR-9 (May 1963), 61 p, Quartermaster Research and Engineering Center, Natick, Mass.**
- 2. C. E. Peters and S. Wehofer, "A General Investigation of Two-Stream Supersonic Diffusers", Tech. Documentary Rept. AEDC-TDR-62-22 (March 1962), 88 p, Arnold Engineering Development Center, Arnold Air Force Station, Tenn.**
- 3. Harold J. Hoge, Suzanne S. Eichacker, and David L. Fiske, "Studies of Jet Compression - 1. Apparatus and Methods. Results with Air at Room Temperature", J Basic Engineering, Trans Am Soc Mech Engrs D81, 426-32 (1959).**
- 4. Suzanne S. Eichacker and Harold J. Hoge, "Jet-Compressor Efficiencies as Influenced by the Nature of the Driving and Driven Gases", J Aerospace Sci 27, 636-7 (1960).**
- 5. H. Pearson, J. B. Holliday, and S. F. Smith, "A Theory of the Cylindrical Ejector Supersonic Propelling Nozzle", J Roy Aero Soc 62, 746-51 (1958).**